Tuning Circuit for NbN SIS Mixer

V.Yu. Belitsky, E.L. Kollberg
Department of Microwave Technology
Chalmers University of Technology, S-412 96, Göteborg, Sweden

Abstract

NbN SIS junction for mixer application has been investigated theoretically in the frequency band 200-2500 GHz considering the junction as a distributed element. We studied the performance of a distributed NbN SIS mixer regarding its particular RF and IF losses. For NbN material we suggested *resonant* distributed SIS mixer that introduces the self-tuned SIS mixer element. The resonant type distributed SIS mixer is a good choice for NbN mixers since this self-compensated SIS junction tuned to the desirable frequency band is much less sensitive to the embedding circuit impedance. Hence the mixer performance is less sensitive to fabrication accuracy of the tuning circuit and NbN film quality.

Introduction

Increasing surface loss in Nb material in Nb-AlO_x-Nb SIS mixers above the gap frequency (~700 GHz) [1] stimulates the use of NbN SIS junction for THz frequencies. The results of development of NbN thin film technology show that it is possible to fabricate a high quality NbN film with the critical temperature about 16 K and normal state conductivity as high as $\sigma_n \approx 1.67 \times 10^6\ \Omega^{-1} \times m^{-1}$ [2]. Different types of SIS junctions based on NbN material were fabricated, *i.e.*, NbN-MgO-NbN and NbN-AlN-NbN tunnel junctions [3-5] with the performance suitable for an application as submm SIS mixers.

The NbN SIS mixer was successfully demonstrated at frequencies about 100 GHz [6]. However at SubMM wavelengths the results of the NbN mixer are less impressive [7]. Reference [8] gives the discussion of problems associated with using NbN SIS junctions and tuning circuits at 630 GHz. The penetration depth (large for NbN material) and associated kinetic inductance makes the tuning circuit design difficult to realise and puts critical constraints on alignment during fabrication of NbN circuits with NbN-MgO-NbN SIS junctions [8].

The NbN films in some cases can demonstrate semiconductor behaviour of conductivity σ_n, as a function of temperature (decreasing σ_n for lower temperatures) [9]. In [10] it was experimentally demonstrated that NbN microstrip tuning circuits have more RF loss compare to Nb-based circuits. However in this work we assumed that NbN film is a superconducting metal well described by the Mattis-Bardeen theory.

The main objective of our work is to develop a new approach to an integrated tuning for the intrinsic capacitance of NbN SIS junction to use in SIS mixers at frequencies 700-1200 GHz. We used modelling to describe material and RF properties of NbN film and employed the

Mattis-Bardeen theory of skin-anomalous effect to predict the performance of the tuning circuit at these frequencies.

NbN films: material and RF properties

The main material parameters that we need to describe a superconductor at high frequencies as an element of RF circuitry are the following: the London penetration depth (λ_o), the gap energy (Δ) at T=0 K, the critical temperature of superconducting transition (T_c) and normal state conductivity (σ_n). Moreover these parameters are related as described in [11, 12]. To define the material it is enough to know λ_o and T_c, while estimated Δ and σ_n can be compared to the measured value with corresponding iteration for the accurate material description. We have chosen the values of these parameters based on data presented in references [2, 3, 7, 8]. The NbN film parameters are listed in Table 1.

It is important that indirect measurement of the penetration depth involving RF resonance can give overestimated values, especially for NbN material due to the large penetration depth compared to the film thickness. In Figure 1 we show the dependence of the effective penetration depth, λ_{RF}, calculated from the RF surface impedance of NbN film (calculated using the Mattis-Bardeen theory) as a function of frequency and the NbN film thickness. The effective penetration depth makes direct impact into the performance of RF lines used to tune out a SIS junction capacitance. The important conclusion from the Figure 1 data is that we must use very thick NbN films for the SIS mixer tuning circuitry ($\approx$1 μm, 2-3 times λ_o) to reduce circuit dependence on the NbN film thickness. Alternatively one can employ relatively thin NbN films with the increased effective penetration depth and with correspondingly higher kinetic inductance of such a film. The latter makes the NbN circuit sensitive to the film thickness and increases the slow-wave factor finally providing critical constrains for the circuit dimension accuracy. In practice the circuit with $\approx$1 μm thick film can be very difficult to fabricate (problems with lift-off process, the layer steps, etc.). In the modelling we used NbN film thickness 400/500 nm (Table 1).

NbN SIS Junction

The large London penetration depth and the thin NbN films with the thickness $\approx \lambda_{RF}$ cause the high kinetic inductance and lead to a very high slow-wave factor value in NbN based strip lines. At frequencies above 700 GHz, where NbN SIS mixer applications are the most interesting, the tuning circuit dimensions become very small because of high frequency and the high slow-wave factor of NbN circuitry. In this condition a small element as for instance μm-size SIS junction has to be considered as distributed element [13, 1].

We based the calculations on the model of NbN-MgO-NbN SIS junction. The junction capacitance as a function of the critical current density was estimated using data from [3].

Figure 2 shows the current-voltage characteristic (IVC) for such a junction. Table 2 lists data for the model of the SIS junction, *i.e.*, the junction quality parameter, leakage-to-normal state resistance ratio (Rj/Rn), the gap voltage V_g, the gap voltage "width" ∂V_g and specific junction capacitance C_c.

Topology of the SIS tunnel junction looks like a plane capacitor. The two superconducting electrodes are separated by the thin (about 1 nm thick) tunnel barrier insulator and the counter electrode is usually more narrow than the base electrode to prevent parasitic capacitance. This topology is the same as for the microstrip line (Figure 3) where the tunnel barrier is interpreted as the insulator [14]. However in contrast to an ordinary microstrip line the insulator is relatively transparent to RF current causing RF loss and the transmission line is non-linear because of the non-linear SIS junction current–voltage characteristic. On this basis we can introduce the electrically long NbN SIS junction as a Superconductor–Insulator–Superconductor Tunnel Strip Line (SIS TSL).

The impedance per unit of length of NbN SIS TSL, Z, includes the surface impedance of the superconducting strip Z_{ss} and the ground plane electrode Z_{sg} (Figure 4), which introduce additional frequency dependent inductance and surface loss [1]. However to find the specific series inductance L and capacitance C of a unit of line one needs to know the thickness of the tunnel insulator s. This is a problem because of the high uncertainty and difficulty of direct measurement of s. We solved this problem empirically by using data for the specific NbN SIS junction capacitance C_C [3]. Then for a NbN-MgO-NbN junction C_C can be approximated as:

$$C_c = \frac{0.36}{\log_e(R_n \cdot A)} \qquad (1),$$

where C_C is the specific capacitance [pF/μm^2], R_n is the junction normal state resistance, [Ω], and A is the junction area [μm^2]. The specific capacitance can also be expressed as a function of the barrier thickness s:

$$C_c = \varepsilon_o \varepsilon_r / s \qquad (2),$$

where ε_0 is the vacuum permitivity and ε_r is the relative dielectric constant of the tunnel barrier material. We used the relative dielectric constant for MgO ε_r=9.6. The barrier thickness s can be estimated for a junction using (1, 2) and data about the junction normal state resistance (measured IVC) and its area.

For the SIS TSL quasiparticle loss, i.e., the loss due to the RF current through the tunnel barrier, is described [15] by:

$$R_{RF}^{mixer} = \{\tfrac{e}{2\hbar\omega} \sum_{n=-\infty}^{\infty} [J_n^2(\alpha) + J_{n-1}(\alpha) \cdot J_{n+1}(\alpha)] \cdot [I_{dc}(U_{bias}^{mix} + (n+1)\hbar\omega / e) + I_{dc}(U_{bias}^{mix} + (n-1)\hbar\omega / e)]\}^{-1} \qquad (3).$$

Here R_{RF}^{mixer} is the impedance for the signal frequency ω_S at a bias voltage U_{bias}^{mix} and LO power given by the LO power normalised parameter α. Here $\alpha=eV_{rf}/\hbar\omega_{lo}$, V_{rf} is the LO amplitude across the junction at the angular frequency ω_{lo}, e is the electron chage and $\hbar$ is the Plank's reduced constatnt. $J_n(\alpha)$ is the Bessel function of the order n, $I_{dc}(U)$ is the DC current-voltage characteristic per unit area of SIS TSL, $\alpha_{lo}\approx 1$ corresponds to the optimum LO power level per unit area of SIS TSL. U_{bias}^{mix} is chosen to be at the middle of the first quasiparticle step below the gap voltage. In (3) we assumed the *SIS TSL* mixer operates with matched RF input.

For any particular junction geometry (the junction area) one can find the SIS TSL specific inductance and capacitance using data from *IVC* DC measurements (Δ, R_n) and employing expressions (1), (2) and (3) and following the procedure described in [1].

As we mentioned above at high frequency (>700 GHz) the wavelength is small. The NbN material properties increase the slow-wave factor so finally a geometrically small size element becomes electrically large, *i.e.*, comparable with the wavelength. In these circumstances we suggest to use a distributed SIS mixer with employing of an internal **resonance** in the electrically long junction [16] as a self-compensated element.

Resonant Distributed SIS Mixer

The effect of the distribution in the NbN SIS junction is clearly observed at Figure 5. To resonate out the intrinsic junction capacitance the length of the junction, L_j, has to be $L_j=n\times\Lambda/4$, where Λ is the wavelength of the signal in the junction *SIS TSL*. The junction width must be small ($\leq\Lambda/6$) to prevent transverse mode propagation.

A distributed SIS mixer element has **intrinsic loss** at RF and IF that originates inherently from the distributed conversion. The SIS mixer performance is a function of LO power [15]. In the case of the mixer feeding through one side (in-line, Figure 6a) the RF power decreases along the SIS TSL mixer, which means that the part of the junction at some distance away from the RF power feeding point is out of optimum operation. For the distributed resonant type SIS mixer this problem can be solved by keeping the resonant length at minimum, for example, $L_j=\Lambda/4$ or $L_j=\Lambda/2$. The first choice gives the shortest possible junction however the distributed mixer input impedance is very low and can be difficult to match with a wave guide or quasioptical system. The half-wave length mixer has a high input real impedance at the expense of higher loss due to **LO power out-of-optimum operation**. Alternatively the resonant $\Lambda/2$ distributed mixer can be fed from both sides by anti-phased signal (as in the double-slot antenna SIS mixer [13]). The two waves injected from both sides of the distributed SIS junction mixer (Figure 6b) will cancel each other at the middle point of the junction, while LO power distribution will be close to that of the $\Lambda/4$ resonant mixer. At IF both sides of the

distributed mixer will work synchronously when LO and signal are shifted by π at every point along the distributed SIS mixer.

A distributed mixer can cause **IF phase-loss** particularly when the mixer length is comparable with IF wavelength in the junction. This loss originates from the phase difference between LO and signal acquired while LO and signal waves are propagating along the junction. For instance the length of about 20 μm for an NbN distributed mixer corresponds to approximately $\Lambda_{IF}/4$ (for the IF frequency 4 GHz). It means that different segments of the distributed mixer will produce IF signals with the phase continuously changing in the range 0-90° with a maximum loss of 3 dB. Simple calculation (omitted here) shows that the upper intermediate frequency in a distributed mixer is limited by in-phase IF operation, the condition of low IF phase-loss is $L_j << \Lambda_{IF}$.

At frequencies above $\approx 1.1 \cdot F_g$ increasing surface loss (Figure 5) suppress resonance. Hence a distributed *SIS TSL* mixer is inherently limited for operation below the gap frequency by the **increasing surface losses** in the superconducting electrodes above the gap frequency (Figure 7). To get rid of the surface loss influence at above NbN gap frequency the SIS junction dimensions have to be smaller than the wavelength, *i.e.,* to be at sub-micron scale.

Resonant Distributed NbN SIS Mixer Tuning Circuit for 1 THz

Usually a tuning circuit for SIS mixer resonates out the junction capacitance and matches the impedance of the wave-guide / quasioptical system to the junction. In the case of the resonant distributed SIS mixer the junction is the self-compensated element (at certain frequency band) and has a reasonable value of real impedance around resonance frequency. The junction can be connected to the LO/ signal source directly or through a matching circuitry to couple to wave-guide mount or antenna impedance. Figure 8 presents schematically the tuning circuit with one step microstrip transformer and NbN resonant distributed SIS mixer in insert and shows the circuit coupling efficiency with the load corresponding to the free space impedance (377 Ω). Table 3 lists circuit dimensions and the NbN SIS junction parameters.

To check the stability of the proposed tuning circuit for the NbN film quality, *i.e.,* changes of the London penetration depth and the accuracy of circuit dimension during fabrication, we made calculations of the circuit coupling efficiency assuming the deviation in the mentioned above parameters. The results of the circuit modeling are presented in Figures 9a, 9b, 9c, 9d.

As the alternative to the resonant type distributed SIS mixer, in [17] the distributed Nb-AlO_x-Nb mixer of another *absorbing* type was suggested and experimentally measured with good results near 460 GHz. In the mixer, according to [17], the RF traveling wave is exponentially absorbed and the reflected power is small. This mixer introduces the electrically long SIS junction with the length of 40 μm that is about 2.5Λ at 460 GHz (the center of the mixer band). To make the input impedance of such a mixer reasonably high to match it with the embedding

circuit, the SIS junction width was narrow 0.15 μm yielding a 13 Ω the transmission line impedance. In such a mixer it appears to be important to consider RF conversion loss due to that different parts of the mixer definitely operate at different LO power levels. The long junction (40 μm) also limits the upper IF frequency (IF phase loss). This tuning circuit requires E-beam lithography for the junction fabrication at the relatively low frequency where other tuning circuits provide competitive performance [13] and employing only photolithography process.

Discussion

The suggested resonant distributed NbN-MgO-NbN mixer has promising features. Below the NbN gap frequency the self-compensated SIS junction in combination with the NbN microstrip transformer/feeder line can produce very stable tuning of the SIS junction intrinsic capacitance in the frequency band of about 200 GHz at the center frequency 1 THz with a coupling efficiency above 0.4.

The resonant type distributed SIS mixer of a quarter or half wavelength long minimises the intrinsic loss of a distributed SIS mixer namely RF conversion loss due to non-equal distribution of LO power and loss due to the phase difference between LO and signal along a distributed junction. The relatively small junction area of a self-compensated SIS mixer keeps the overall junction capacitance low which eliminates IF coupling loss. Our analysis shows that above the gap frequency a distributed SIS mixer will have very high conversion loss due to increasing surface loss in superconducting electrodes.

We suggest the two coupling schemes of the resonant distributed SIS mixer which can be employed for wave-guide and quasioptical mixers. The feeding from both sides by anti-phase signal is suitable for the double-slot or double-dipole antenna quasioptical mixers while the one side feed scheme fits a waveguide or the spiral antenna configuration. According to the modelling the variations of either NbN film quality or the tuning circuit dimensions produce minor change in the tuning band and the coupling efficiency.

Acknowledgements

Dr. S.A. Torchinsky (University of Calgary) is greatly appreciated for reading the manuscript and many useful comments. We also acknowledge the Swedish National Board for Industrial and Technical Development and the Swedish National Space Board for financial support.

References

[1] V.Yu. Belitsky, S. W. Jacobsson, L.V. Filippenko, E.L. Kollberg, "Theoretical and Experimental Studies of Nb-based Tuning Circuits for THz SIS Mixers", *Proc. of Sixth Int. Symp. on Space Terahertz Technology*, pp. 87-102, March 21–23 (1995), California Institute of Technology, Pasadena, USA.

[2] R.E. Treece, J.S. Horwitz, J.H. Claassen, D.B Chrisey, "Pulsed laser deposition of high-quality NbN films", *Appl. Phys. Lett.* **65** (22), pp. 2860-2862, 28 November 1994.

[3] J.A. Stern, H.G. LeDuc, A.J. Judas, "Fabrication and Characterisation of High Current-Density, Submicron, NbN/MgO/NbN Tunnel Junctions", *Proc. of Third Int. Symp. on Space Terahertz Technology*, pp. 420-438, March 24–26 (1992), Univ. of Michigan, Ann Arbor, USA.

[4] M.Aoyagi, H. Nakagawa, I. Kurosava, S. Takada, " NbN/MgO/NbN Josephson Junctions for Integrated Circuits", *Jpn. J. Appl. Phys.*, **31**, Part 1, No.6A, pp.1778-1783, June 1992.

[5] Z. Wang, A. Kawakami, Y. Uzawa, B Komjyama, " High critical current density NbN/AlN/NbN tunnel junctions fabricated on ambient temperature MgO substrates", *Appl. Phys. Lett.* **64** (15), pp. 2034-2036, 11 April 1994.

[6] A. Karpov, B. Plathner, K.H. Gundlach, M. Aoyagi, S. Takada, "Noise Properties of a Mixer with SIS NbN Quasiparticle Tunnel Junctions", *Proc. of Sixth Int. Symp. on Space Terahertz Technology*, pp. 117-122, March 21–23 (1995), California Institute of Technology, Pasadena, USA.

[7] Y. Uzawa, Z. Wang, A. Kawakami, B. Komjyama, "Submillimeter wave responses in NbN/AlN/NbN tunnel junctions", *Appl. Phys. Lett.* **66** (15), pp. 1992-1994, 10 April 1995.

[8] M. Salez, J.A. Stern, W.R. McGrath, H.G. LeDuc, "NbN Mixers and Tuning Circuits for 630 GHz: Design and Preliminary Measurements", *Proc. of Sixth Int. Symp. on Space Terahertz Technology*, pp. 103-116, March 21–23 (1995), California Institute of Technology, Pasadena, USA.

[9] J.-H. Tyan, J.T. Kue, "Grain boundary scattering in the normal state resistivity of superconducting NbN thin films", *J. Appl. Phys.* **75** (1), pp.325-331, 1 January 1995.

[10] W.R. McGrath, J.A Stern, H.H.S. Javadi, S.R. Cyper, B.D. Hunt, H.G. LeDuc, "Performance of NbN superconductive tunnel junctions as SIS mixer at 205 GHz", *IEEE Trans. Mag.*, **MAG-27**, pp. 2650-2653, (1991).

[11] R.L. Kautz, "Picosecond pulses on superconducting striplines," *J. Appl. Phys*, Vol. **49** (1), pp. 308-314, 1978.

[12] R. Pöpel, "Surface impedance and reflectivity of superconductors," *J. Appl. Phys*, **66** (12), pp. 5950-5957, 1989.

[13] J. Zmuidzinas, H. G. LeDuc, J. A. Stern, and S. R. Cypher, "Two-Junction Tuning Circuits for Submillimeter SIS Mixers," *IEEE Trans. on MTT*, Vol. 42, pp. 698-706 (1994).

[14] J.C. Swihart, "Field solutions for a thin film superconducting strip transmission line," *J. Appl. Phys*, Vol. 32, pp. 461-469 (1961).

[15] J.R. Tucker, M.J. Feldman, "Quantum detection at millimeter wavelengths", *Rev. of Modern Phys.*, Vol. 4, pp. 1055–1113 (1985).

[16] V.Yu. Belitsky and E.L. Kollberg, "Superconductor–Insulator–Superconductor Tunnel Strip Line: Features and Applications", *To appear in Journal of Applied Physics*, 1996.

[17] C.E. Tong, R. Blundell, B. Bumble, J.A. Stern, H.G. LeDuc, "Quantum Limited Heterodyne Detection in Superconducting Non-Linear Transmission Lines at Sub-Millimeter Wavelengths", *Applied Physics Lett.*, **67** (9), pp.1304-1306 August 28, 1995.

Tables

Table 1. NbN film material parameters used in the modelling

London penetration depth λ_o, [nm]	Gap energy Δ/e, [mV] (at T=0 K)	Critical temperature T_c, [K]	Normal state conductivity, σ_n, [$\Omega^{-1}\times m^{-1}$]
280	4.46	16	9.55×10^5
NbN film thickness, [nm]			
Base electrode: 400		Top electrode: 500	

Table 2. IVC parameters for NbN-MgO-NbN SIS junction used in the modelling.

Leakage-to-normal state resistance ratio (Rj/Rn)	Gap voltage V_g, [mV] at 4.2 K	Gape voltage "width", ∂V_g, [mV]	Specific junction capacitance C_c, [pF/μm^2], for J_c=20 kA/cm^2
10	4.45	0.445	0.12

Table 3. The tuning circuit dimensions and SIS junction parameters.

Microstrip transformer dimensions, [μm]				
Strip width	Transformer length	Ground electrode thickness	Strip electrode thickness	Insulator thickness (SiO)
1,0	21,0	0.4	0.5	0.5
Distributed SIS junction parameters and dimensions				
Junction length, [μm]	Junction width, [μm]	Junction RnA, [Ωμm^2]	Ground electrode thickness, [μm]	Counter electrode thickness, [μm]
1.5	0.5	15	0.4	0.5

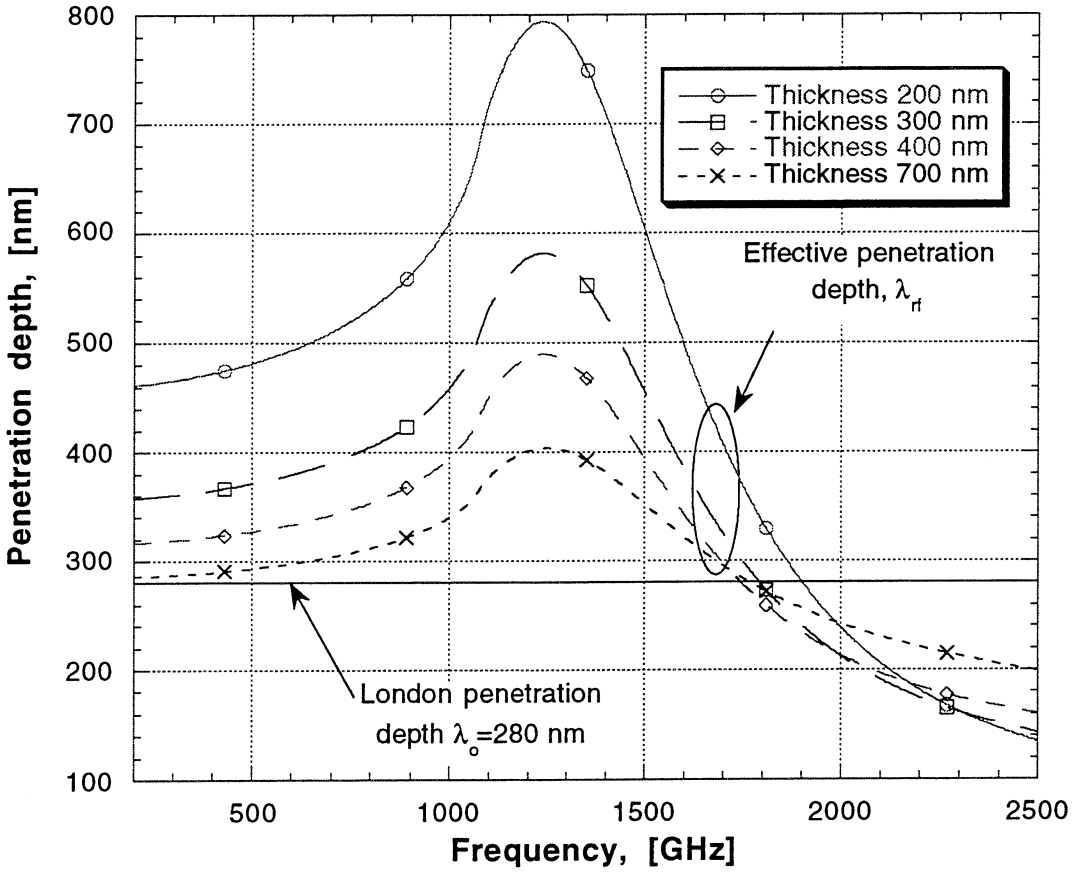

Figure 1. The effective penetration depth of NbN film (estimated from the surface impedance) is plotted *vs.* frequency. The NbN film surface impedance was calculated based on the Mattis-Bardeen theory. We used the NbN material parameters listed in Table 1. The effective penetration depth, λ_{rf}, demonstrates strong dependence on the frequency above 500 GHz and hence a NbN microstrip line is dispersive above this frequency. The NbN film thickness must be of the order 2-3 λ_o to decrease the slow-wave factor (~λ_{rf}). To have the RF properties of the NbN film less dependent on the film thickness and to pick the processing restrictions on the fim thickness (possibility of lift-off, layer steps) we used 400 and 500 nm NbN thick film for the bottom and the top electrodes in the modelling of the tuning circuit.

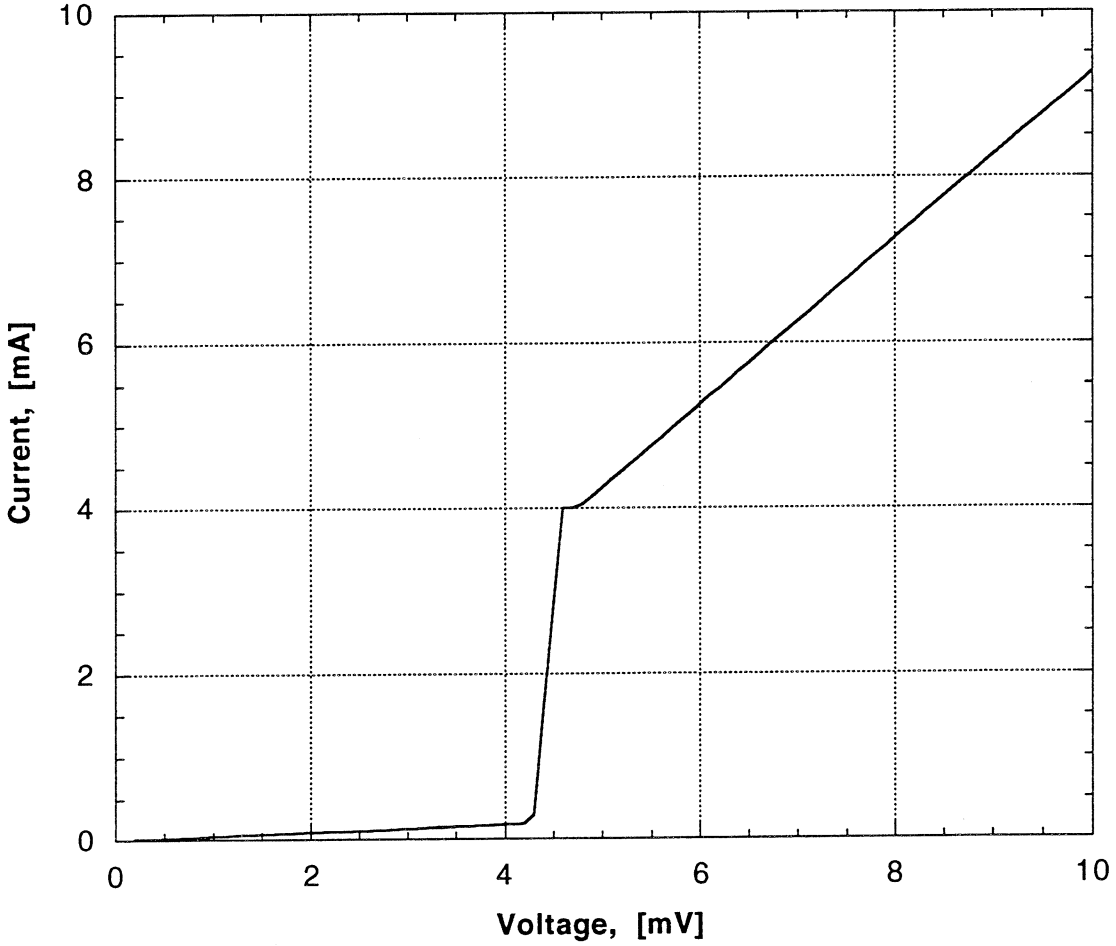

Figure 2. The model current voltage characteristic (IVC) for NbN-MgO-NbN SIS junction. The IVC was used in the modelling to calculate the SIS junction RF impedance according to the Tucker-Feldman theory. The junction IVC parameters are listed in Table 2. The model IVC was scaled at the current according to the choice of the critical current density. The gap voltage changes according to the BCS theory at the different temperatures.

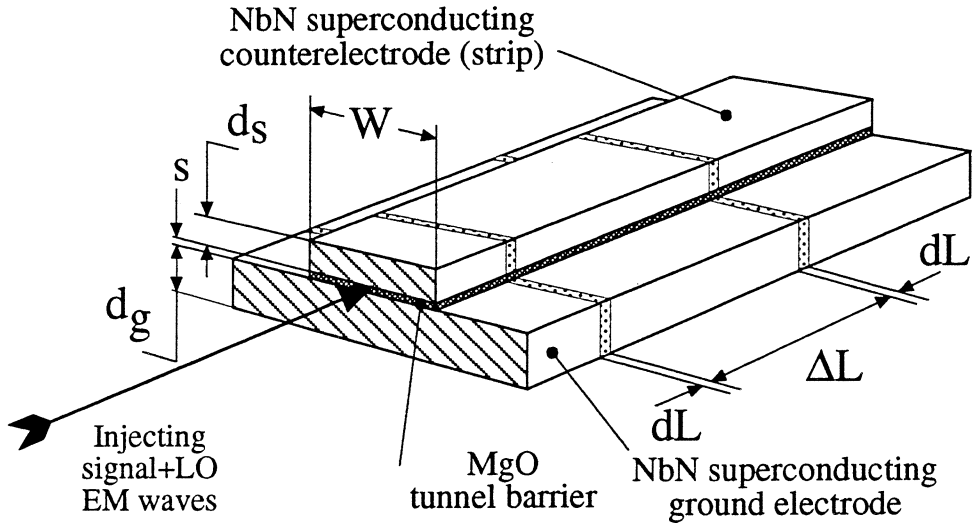

Figure 3. Schematic drawing of a NbN-MgO-NbN SIS junction that illustrates topological similarity of a SIS junction and a microstrip line. In the modelling we described the SIS junction as a segment of microstrip transmission line. We assumed that at the high frequencies (above 500 GHz) the wavelength is short and the slow-wave factor in the NbN strip line circuitry is high. In these conditions the NbN junction of a few μm size (≤ 5 μm) already demonstrates resonant behaviour in 200-1140 GHz frequency band (see also Figure 5).

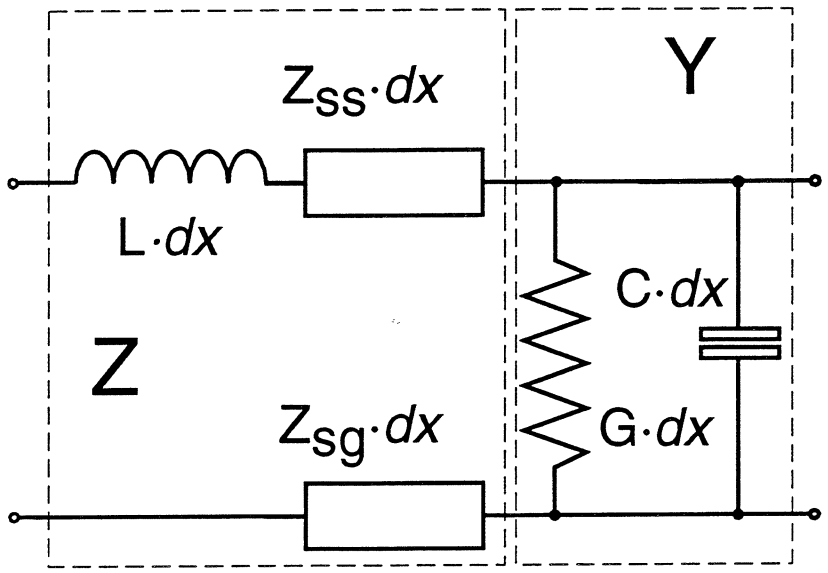

Figure 4 Circuit diagram for the unit of length of a superconductor-insulator-superconductor tunnel microstrip line. *L, C* are specific geometrical inductance and capacitance per the unit length; Z_{ss}, Z_{sg} are the surface impedance of microstrip and ground electrodes respectively, calculated according to the Mattis-Bardeen theory; $G=1/R_{RF}^{mixer}$ is the quasiparticle quantum non-linear conductance per unit of SIS junction line.

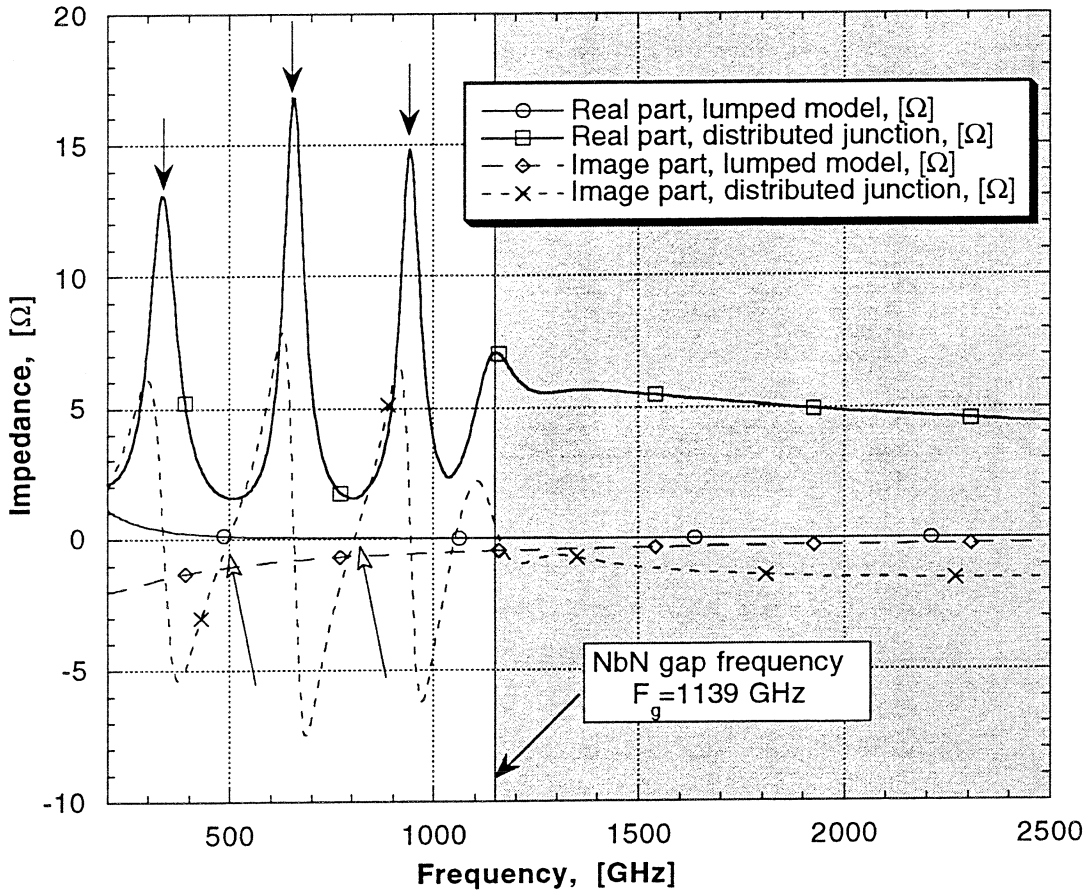

Figure 5. The imaginary and real parts of the input impedance of NbN-MgO-NbN SIS junction. The junction parameters used in the modelling: the junction size $0.5\times5.0\ \mu m^2$, the junction normal state resistance Rn=8 [Ω], other parameters are listed in Tables 1, 2 . At the plot we present results of the modelling for the lumped model ($R_{rf}||C$) and the distributed model. In the latter case the junction is considered as a segment of the transmission line with the open end. The effect of distributed behaviour can be observed at several resonance frequencies. The series resonance, the junction length $L_j=(2n+1)\Lambda/4$, is indicated by the open head arrow. While for the parallel resonance having higher the real part of the impedance, the junction length is $L_j=2n\Lambda/4$. Those frequencies are marked by filled head arrow. Above the gap frequency, resonance is completely suppressed by increasing surface loss in the superconducting electrodes (see also Figure 7).

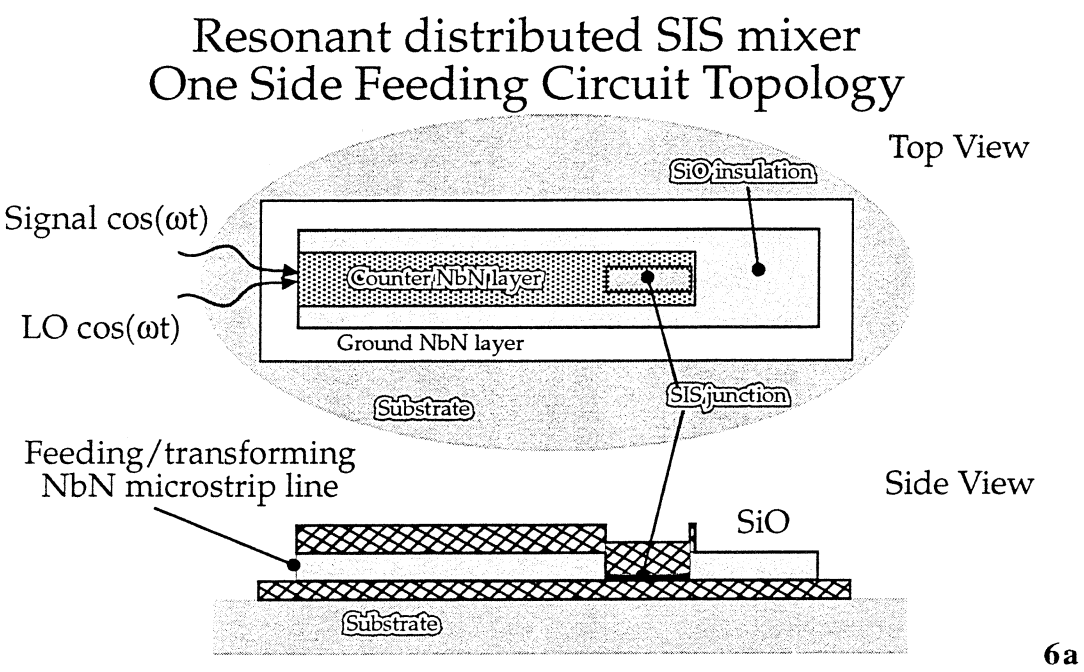

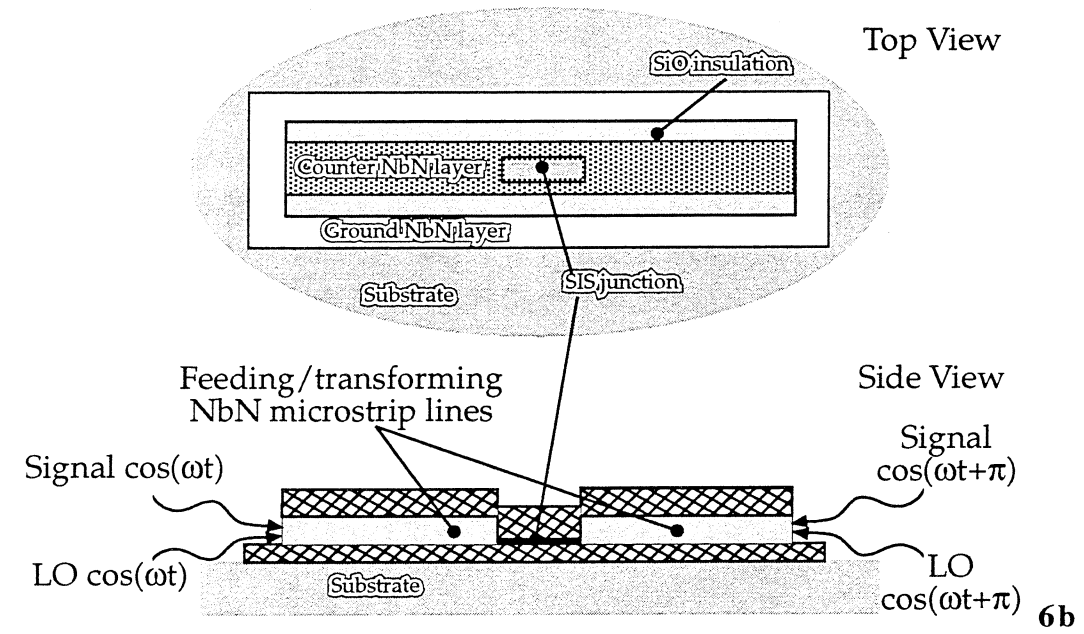

Figure 6a,b. Schematic drawing of the tuning circuit employing self-compensated SIS junction. The drawing presents only RF feed scheme. DC bias is not shown for clarity. *Figure 6a*, LO and signal are injected via the microstip feed line that couples the power to the distributed SIS junction from one side while another side of the junction is open. *Figure 6b*, LO and signal are injected via both sides (with 180° phase shift) of the distributed resonant mixer and cancel each other at the middle point of the symmetrical circuit. In the modeling we neglected discontinities of the feeding microstrip line—to—the SIS line connection.

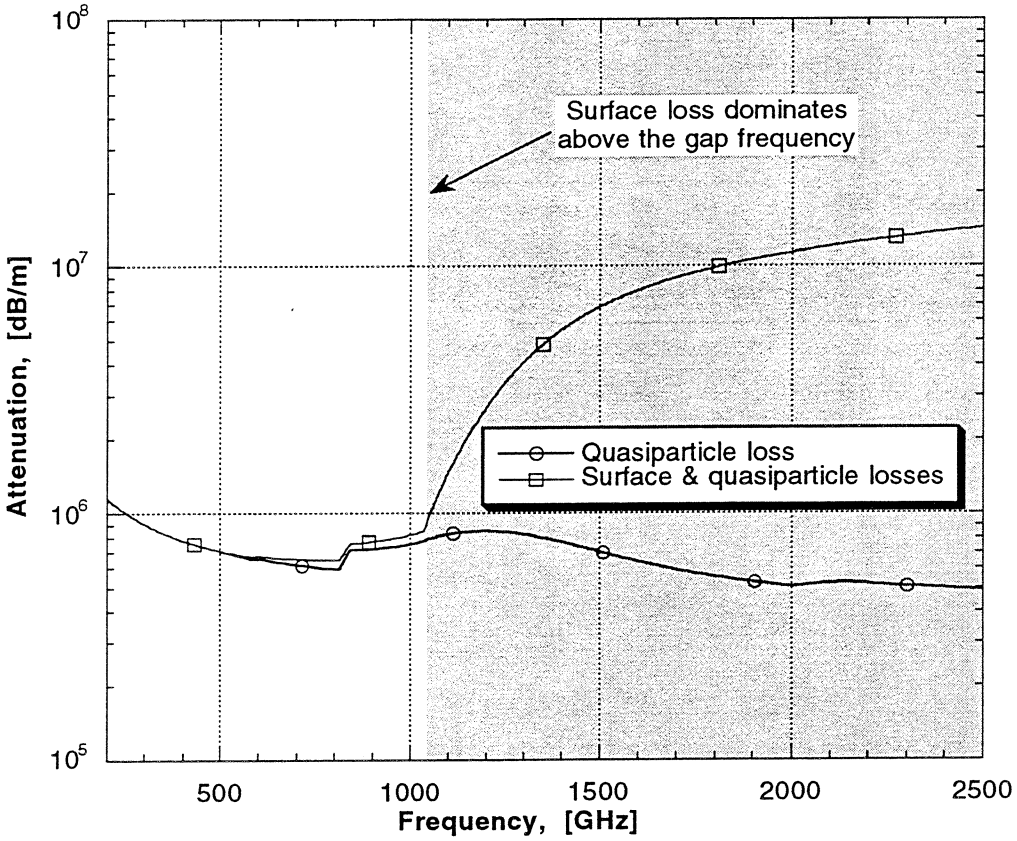

Figure 7. Attenuation in the NbN-MgO-NbN SIS junction transmission line for the signal frequency. The modelling was made for the LO power normalised value α=1,0, the ambient temperature 8 K, the SIS junction normal state resistance — junction area product, RnA=15 [$\Omega\times\mu m^2$]. Increasing the surface loss above the gap frequency causes suppression of the resonance in the distributed SIS junction (see also Figure 5). Above the gap frequency a distributed SIS mixer has very high conversion loss due to the signal dissipation in the electrodes.

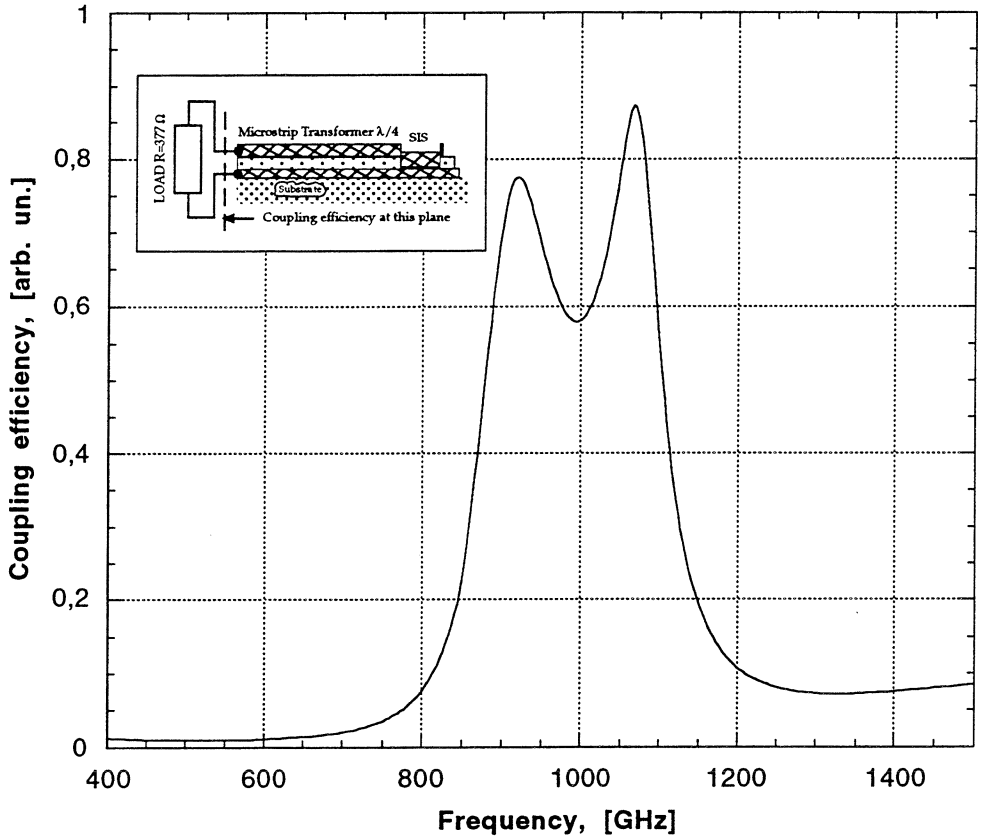

Figure 8. The plot shows the coupling efficiency of the tuning circuit drawn in the insert, *i.e.*, the resonant distributed NbN-MgO-NbN SIS mixer with one side feed through the λ/4 microstrip transformer. The circuit dimensions and the SIS junction parameters are presented in Table 3.

See Figure 9a, 9b, 9c, 9d on the next two pages.

Figure 9. At the Figure 9 we show the results of our testing of the tuning circuit stability. We changed the parameters of NbN material and the tuning circuitry geometry and the SIS junction parameters typically with the increment ±10% of the values presented in the Table 3. Figure 9a shows the result of the change in the transformer microstrip width. At Figure 9b we present the effect of the change in the microstrip transformer length. Figure 9c presents the result of the change in the distributed SIS junction length (the most critical parameter affecting on the tuning frequency). The plot Figure 9d shows the effect of the change in NbN material penetration depth. Data presented on Figure 9a, 9b, 9c,9d demonstrates that the suggested circuit is reasonably stable concerning accuracy of fabrication and stability of NbN material quality.

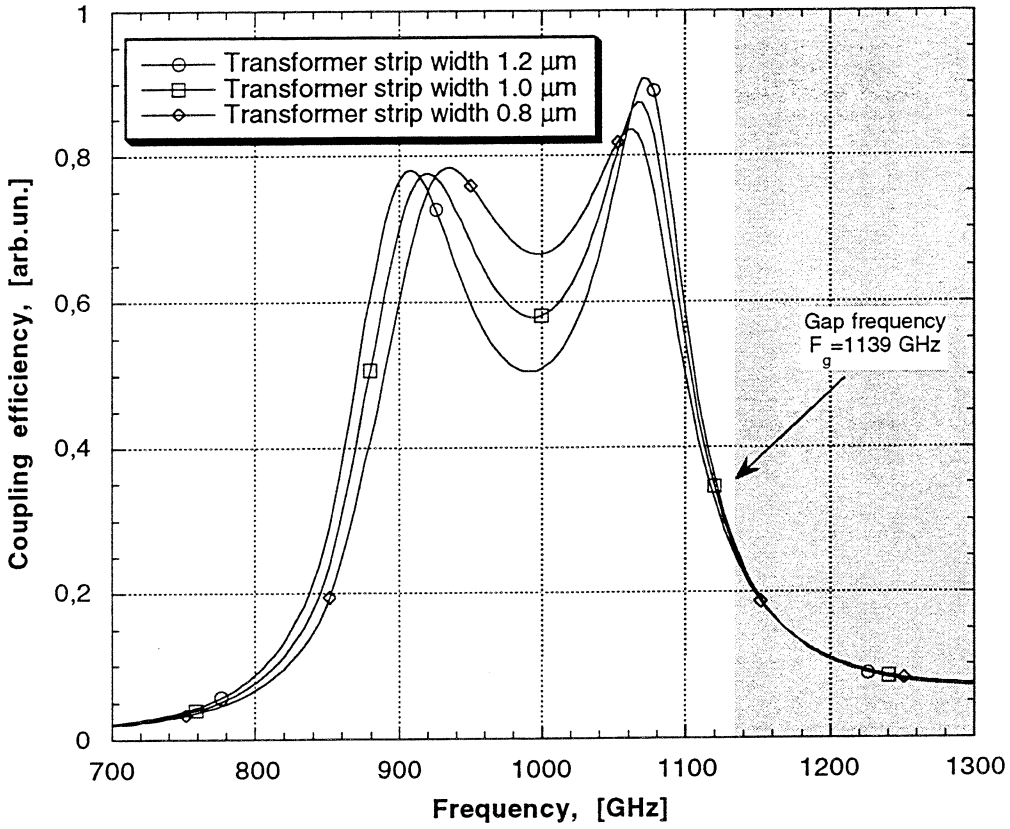
Transformer strip width 1.2 μm
Transformer strip width 1.0 μm
Transformer strip width 0.8 μm
Gap frequency
F g =1139 GHz
Coupling efficiency, [arb.un.]
Frequency, [GHz]
0
0,2
0,4
0,6
0,8
1
700
800
900
1000
1100
1200
1300

9a

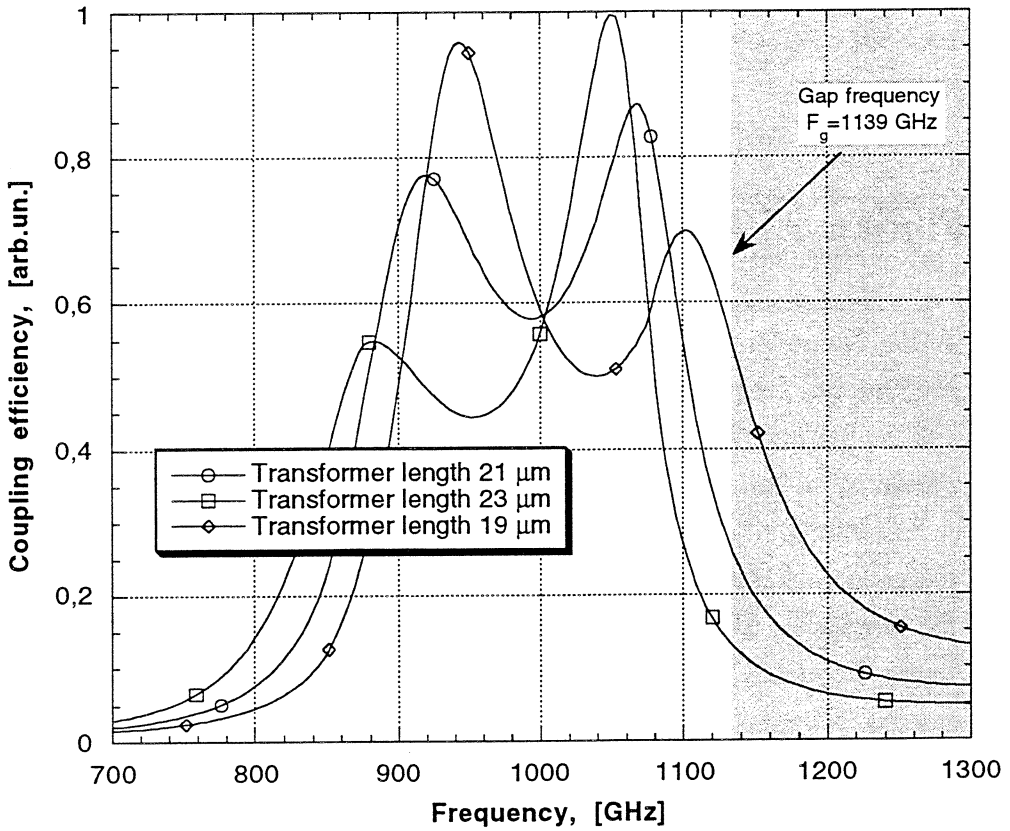
Gap frequency
F g =1139 GHz
Transformer length 21 μm
Transformer length 23 μm
Transformer length 19 μm
Coupling efficiency, [arb.un.]
Frequency, [GHz]
0
0,2
0,4
0,6
0,8
1
700
800
900
1000
1100
1200
1300

9b

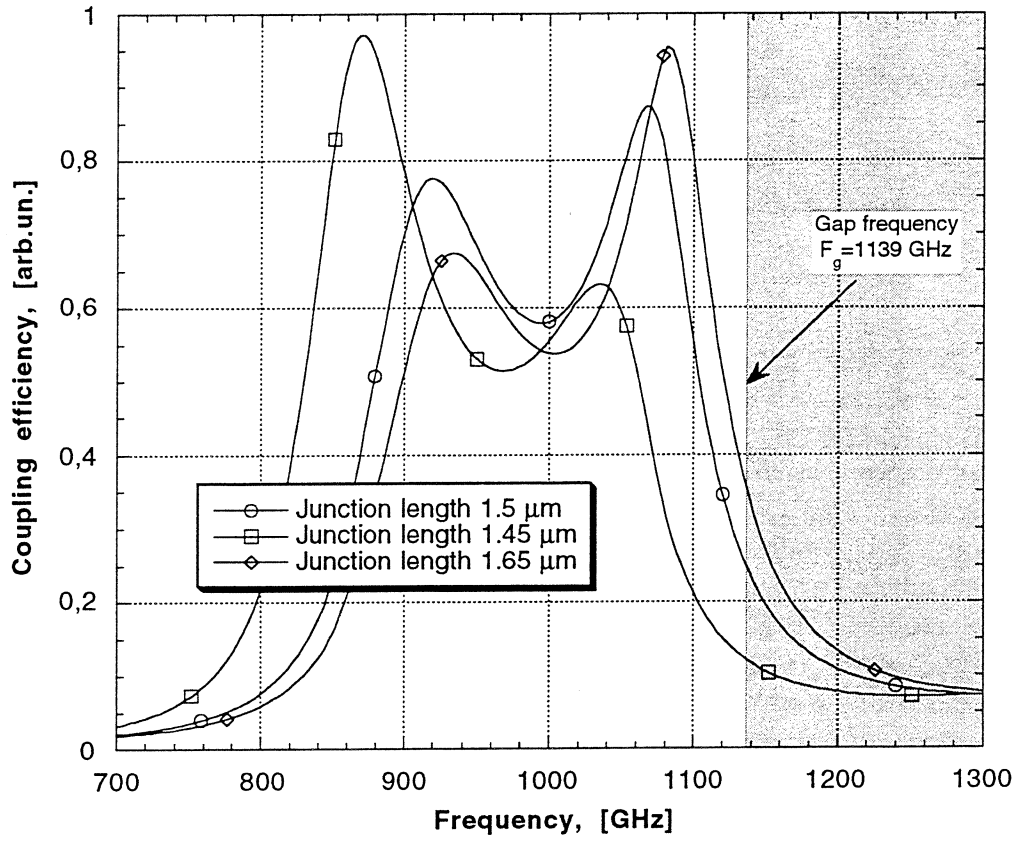
Coupling efficiency, [arb.un.]
Frequency, [GHz]
Gap frequency
F_g=1139 GHz
Junction length 1.5 μm
Junction length 1.45 μm
Junction length 1.65 μm
0
0,2
0,4
0,6
0,8
1
700
800
900
1000
1100
1200
1300

9 c

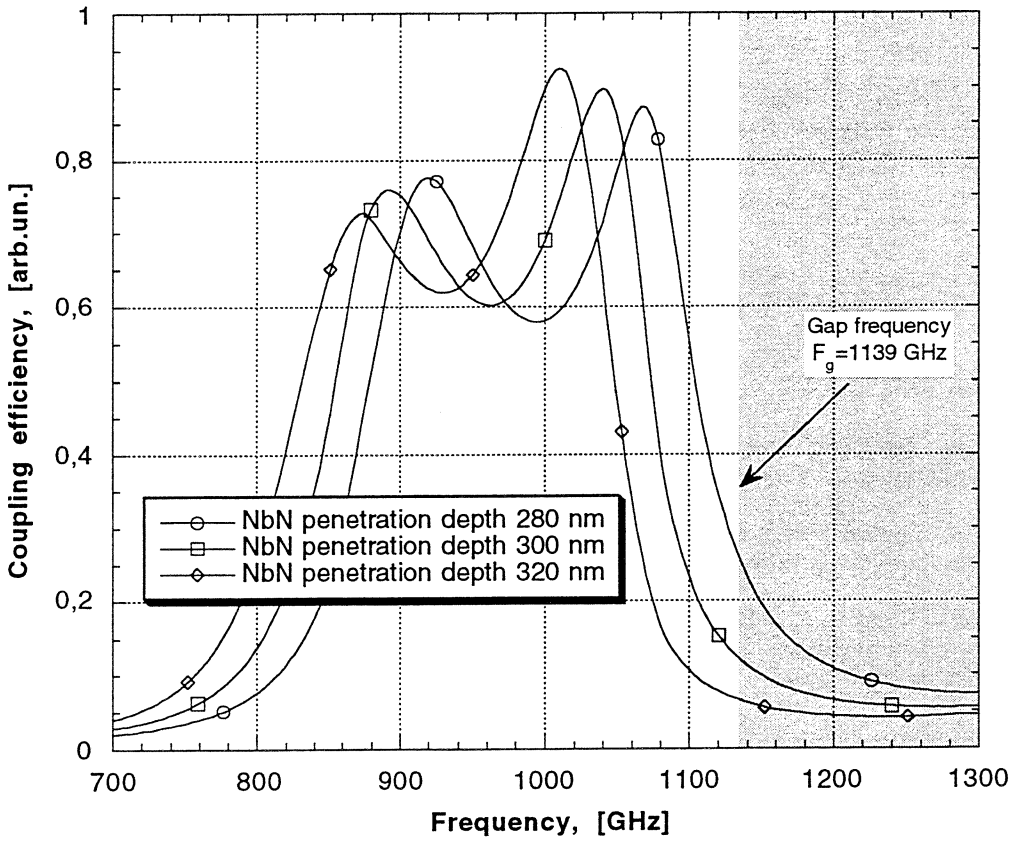
Coupling efficiency, [arb.un.]
Frequency, [GHz]
Gap frequency
F_g=1139 GHz
NbN penetration depth 280 nm
NbN penetration depth 300 nm
NbN penetration depth 320 nm
0
0,2
0,4
0,6
0,8
1
700
800
900
1000
1100
1200
1300

9d